HHS Public Access

Author manuscript

J Neurosci Methods. Author manuscript; available in PMC 2017 April 01.

Published in final edited form as:

J Neurosci Methods. 2016 April 1; 263: 57–67. doi:10.1016/j.jneumeth.2016.01.025.

A flow cytometeric approach to analyzing mature and progenitor endothelial cells following traumatic brain injury

Poincyane Assis-Nascimento[1], **Oliver Umland**[2], **Maria L. Cepero**[1], and **Daniel J. Liebl**[1]

[1]The Miami Project to Cure Paralysis, the Department of Neurosurgery, the University of Miami, Miller School of Medicine, Miami, FL, USA

[2]Diabetes Research Institute, the University of Miami, Miller School of Medicine, Miami, FL, USA

Abstract

Background—Traumatic brain injury (TBI) continues to be a major source of death and disability worldwide, and one of the earliest and most profound deficits comes from vascular damage and breakdown of the blood-brain barrier (BBB). Cerebral vascular endothelial cells (cvECs) and endothelial progenitor cells (EPCs) have been shown to play essential roles in vessel repair and BBB stability, although their individual contributions remain poorly defined.

New Method—We employ TruCount beads with flow cytometry to precisely quantify cvECs, EPCs and peripheral leukocytes in the murine cortex after controlled cortical impact (CCI) injury.

Results—We found a significant reduction in the number of cvECs at 3 days post-injury (dpi), whereas the EPCs and invading peripheral leukocytes were significantly increased compared with sham controls. Proliferation studies demonstrate that both cvECs and EPCs are undergoing cell expansion in the first week post-injury. Furthermore, analysis of protein expression using mean fluorescent intensity found increases in PECAM-1, VEGFR-2, and VE-Cadherin expression per cell at 3 dpi, which is consistent with western blot analysis.

Comparison with Exiting Methods—Classic methods of cell analysis, such as histological cell counts, in the traumatic injured brain are labor intensive, time consuming, and potentially biased; whereas flow cytometry provides an efficient, non-biased approach to simultaneously quantify multiple cell types. However, conventional flow cytometry that employs capped events can provide misleading results in CNS injured tissues.

Conclusions—We demonstrate that TruCount quantification using flow cytometry is a powerful tool for quantifying mature and progenitor endothelial cell changes after TBI.

Corresponding Author: Daniel J Liebl, PhD, Professor of Neurological Surgery, The Miami Project to Cure Paralysis, The University of Miami, 1095 NW 14th Terrace, R-48, Miami, FL 33136, Ph# 305 243-7143, Fax# 305 243-3914, dliebl@miami.edu.

Conflicts of Interest: The authors declare no competing financial interests.

Keywords

Flow cytometry; endothelial cells; endothelial progenitor cells; blood vessels; traumatic brain injury

1.1 Introduction

Every year, nearly 2 million individuals are victims of traumatic brain injury (TBI), contributing to over 30% of all injury-related deaths in the United States alone (Centers for Disease and Prevention, 2013). TBI is a multifaceted progressive disorder that can lead to profound neurological deficits that are typically initiated by external mechanical forces to the brain. Acute disruption of the vascular network leads to subdural hematoma, epidural hematoma and/or intraparenchymal hematoma even in some mild TBI cases (Kan et al., 2012). Open head and penetrating wounds can also lead to intracranial hemorrhage as a result of vascular damage in the brain. Even though vessel damage is associated with the majority of TBI patients, our understanding of the mechanism(s) and dynamics of vessel damage, repair, and regeneration are limited.

Normal brain function is dependent on an array of vascular networks to receive an adequate supply of oxygen and nutrients. The blood vessel endothelium is composed of cerebral vascular endothelial cells (cvECs) that form tight junctions and interact with other vascular cells, such as pericytes and astrocytes, and their basal lamina to form a selectively permeable barrier in the central nervous system (CNS) called the blood brain barrier (BBB) (Abbott et al., 2010). TBI can lead to BBB disruption associated with decreased supply of oxygen and nutrients and increased infiltration of circulating elements that includes peripheral cells (Abdul-Muneer et al., 2013). Peripheral cell infiltration can include circulating leukocytes, such as monocytes, macrophages, T-cells, B-cells, and other inflammatory cell types, but also includes circulating endothelial progenitor cells (EPCs) (Das et al., 2012). Increased infiltration of bone marrow-derived EPCs are believed to have beneficial influences on vessel repair and possibly new vessel growth (Guo et al., 2009; Timmermans et al., 2009; Xue et al., 2010); however, the cellular responses of cvECs and peripheral EPCs within the changing TBI environment are complex and remain poorly defined.

Flow cytometry is a rapid, flexible and sensitive technique that allows for detailed simultaneous measurements of diverse cell populations within specific tissues. Flow cytometry utilizes light scatter properties to measure the relative size and internal complexity of particles of interest, while fluorescently labeled dyes or antibodies are used to measure viability, DNA content or protein expression levels (Bendall et al., 2012; Lugli et al., 2010). Less than a decade ago, flow cytometry was a method used primarily in the field of immunology (De Rosa et al., 2001; Perfetto et al., 2004), but has been adopted by multiple fields including neuroscience. In the progressive TBI pathology, flow cytometry can be used to analyze the temporal flux of multiple cell types at a given time point; however, proper identification of the target cell populations becomes challenging as a result of injury-induced environmental alterations that include cell loss, proliferation, differentiation and infiltration. Hence, data interpretation is heavily dependent on the gating

strategy (Mair et al., 2015), inclusion and exclusion markers, as well as single color and isotype controls to provide an adequate assessment of cellular dynamics in TBI tissues. Here, we demonstrate that accurate cell quantification can be achieved in the controlled cortical impact (CCI) injured mouse cortex using measurements based on capped (predetermined number) events in combination with TruCount beads and defined markers for both mature cvECs and infiltrating EPCs to demonstrate the relative contributions of each cell type to CNS injury. Combining this analysis with proliferative markers strengthens our understanding of the environmental contributions that lead to temporal differences in cell numbers.

1.2 Materials and Methods

1.2.1 Animals

Generation of Cdh5-zG mice resulted from crossing Cdh5(pac)-CreERT2 (Tg (Cdh5-cre/ERT2) 1Rha, MGI: 3848982) (Sorensen et al., 2009) with Rosa zGreen reporter mice (007906 B6.Cg-Gt (ROSA) 26Sor<tm6 (CAG-ZsGreen1) Hze>/J; The Jackson Laboratory, Bar Harbor, ME). Thy-1-YFP mice were obtained from Jackson Laboratory (JAX Mice Database - 003782 B6.Cg-Tg (Thy-1-YFP) HJrs/J). All procedures related to animal use and care were approved by the University of Miami Animal Use and Care Committee. Animals were housed in a 12 hour light/dark cycle and food and water were supplied *ad libitum*.

1.2.2 Controlled cortical impact (CCI) injury

Male mice between the ages of 2–4 months were anaesthetized with 100 mg/kg ketamine and 10 mg/kg xylazine by intraperitoneal (i.p.) injections. Using aseptic techniques, a 5 mm craniotomy was made using a portable drill over the right parieto-temporal cortex (−2.5 mm caudal and 3 mm lateral from bregma, epicenter). The injury was generated using a 3 mm beveled stainless steel tip attached to an eCCI-6.3 device (Custom Design & Fabrication), at velocities ranging from 2 to 6 m/s, depth of 0.5 mm deep and 150 ms impact duration. The surgeries for all flow cytometry and western blot studies were performed at a velocity of 4 m/s. After CCI injury the skin was sutured using 5-0 coated vicryl sutures (Ethicon, J391) and animals were placed on a warm heating pad until they recovered from anesthesia. Surgical sham mice received only the opening and re-suturing of the skin.

1.2.3 Histology

Mice were anesthetized and prepared for CCI injury as described above. Animals received intracardiac perfusion with phosphate buffered saline (PBS, pH 7.4) followed by 4% paraformaldehyde (PFA) at 3 and 7 days post CCI injury (dpi). Brains were postfixed in 4% PFA overnight at 4°C, dehydrated in 30% sucrose for 24 h and embedded in clear frozen section compound (VWR, 95057-838) for cryostat sectioning. Thirty micron cryostat sections were stained using a standard hematoxylin and eosin (H&E) histological staining. Slides were rinsed in distilled water for 5 min to remove all section embedding compound then immersed in hematoxylin for 3 min and rinsed again in running distilled water for 5 min. Slides were then immersed in eosin for 30–45 seconds followed by 3 min incubations of increasing ethanol (EtOH) concentrations: 70% EtOH (1X), 95% EtOH (2X), 100% EtOH (2X). Slides were then immersed in methyl Salicylate for 5 min followed by 3 times

in xylene for 3 min. Slides were mounted with a xylene-based mounting medium and samples were imaged using a bright field Olympus BX50 microscope equipped with Olympus SC30 digital color camera and Olympus analysis getIT software for image capturing.

1.2.4 Lectin Infusion

Mice were deeply anaesthetized with 100 mg/kg ketamine and 10 mg/kg xylazine cocktail and intracardiac perfusion was performed with approximately ~50 mL ice cold, filtered PBS to flush blood. Mice were mildly fixed with 1% PFA and then 15 mL of DyLight 594 labeled Lycopersicon Esculentum (Tomato) Lectin (DL 1177; Vector Laboratories, Burlingame, CA), was slowly flushed through the heart followed by 50 mL of ice cold 4% PFA.

1.2.5 THF Dehydration and Tissue clearing for Ultramicroscope Imaging

Brains were post-fixed in 4% PFA overnight in 4°C, protected from light and then washed in PBS for 24 h. Brains were dissected and the ipsilateral injured cortex was placed in a 30 mL glass amber packer bottle (VWR; Suwanee, GA) for the remaining steps. A four-step dehydration procedure was performed with increasing concentrations of tetrahydrofuran (THF) in distilled water: (1) 50% THF for 2 h; (2) 80% THF for 2 h; (3) 100% THF overnight (~16 hours); (4) 100% THF for 24h. All incubation steps were done at 4°C on a shaker. For clearing, the brains were incubated in a 1/3 benzyl alcohol (Sigma-Aldrich, 402834), 2/3 benzyl benzoate (Sigma-Aldrich, B6630) (BABB) solution for 2–4 h (on a shaker at 4°C) prior to imaging. Cleared cortices were imaged on a LaVision BioTec Ultramicroscope based around an Olympus MVX10 zoom microscope body (variable zoom 0.63 – 6.3 X) including light sheet excitation lines OPSL (50mW), 488nm, OPSL (50mW), 561nm and diode laser (50mW), 647nm. The camera used was an Andor Neo scientific low noise sCMOS camera with GFP/FITC: 525/50, TRITC/Alexa594: 620/60 and Alexa 647/Cy5: 700/80 detection channels. 3D image analysis was done using Imaris 8.1.2 (Bitplane) software.

1.2.6 Preparation of Dissociated Cells

Adult male mice (2–4 months) were euthanized and their brains were quickly extracted and placed in cold Hank's Balanced Salt Solution, without calcium chloride, magnesium chloride or magnesium sulfate ($HBSS^{-/-/-}$) (Gibco, 14175). The ipsilateral injured and corresponding sham cortices were dissected, thoroughly minced, centrifuged at 1200 rpm for 5 min and then incubated in an enzymatic solution (Worthington, Lakewood, NJ), containing 30 U/ml papain (Worthington, LK003188) and 40 μg/ml DNase I (Worthington, LK003170) in Earl's Balanced Salt Solution (EBSS) (Worthington, LK003188) for 70 min at 37°C. After incubation the digested brain tissue was homogenized by passing it 10 times through an 18 gauge needle (B-D, 305195) and subsequently 10 times through a 21 gauge needle (B-D, 305165). The homogenized brain cells were then mixed with 1.7 volumes of 22% bovine serum albumin (BSA in PBS pH 7.4) and centrifuged at 2600 rpm for 10 min at 4°C. The myelin/lipid layer on top of the vial was carefully aspirated and discarded, and the cell pellet was washed in 2 mL of Hank's Balanced Salt Solution with calcium and magnesium chloride ($HBSS^{+/+}$) (Gibco, 14025), filtered through the cell-strainer cap of 5mL

polystyrene round-bottom tubes (Falcon, 352235) and centrifuged once more at 1200 rpm for 5 min. Finally, cells were re-suspended in 1 ml of the same $HBSS^{+/+}$ solution for further staining and flow cytometric analysis.

1.2.7 Flow Cytometric Analysis

Homogenized cortical cells were incubated with Live/Dead fixable Near-IR dead Cell Stain Kit (Life Technologies, L10119 Eugene, Oregon, USA) in 1mL $HBSS^{+/+}$ on ice for 30 min, protected from light. Cells were then blocked at 4°C in FcR blocking solution (MACS Miltenyi Biotec, 130-092-575 in 0.5% BSA) for 15 min at 4°C. Fluorescently conjugated antibodies: PE-Cy7 anti-Mouse CD45 (affymetrix eBioscience, 25-0451) 1:100, FITC anti-Mouse CD31 (PECAM-1) (BD Pharmigen, 553372) 1:50, PE anti-Mouse CD133 (Biolegend, 141203) 1:200, BV421 Rat anti-Mouse CD144 (VE-Cadherin) (BD Horizon, 562795) 1:100, all diluted in FcR blocking solution, were used for surface staining by incubating cells for 20 min at 4°C, protected from light. For intracellular staining, cells were fixed for 20 min with 0.5mL Cytofix on ice (BD Cytofix/Cytoperm, 554714) and incubated with anti-mouse vascular endothelial growth factor receptor-2 (VEGFR-2) antibody (CD309 – Cell Sinaling, 2479S) diluted 1:300 in BD perm/wash buffer for 20 min at room temperature (RT), protected from light. Cells were centrifuged at 1200 rpm for 5 min, washed with BD perm/wash buffer and incubated at RT in donkey anti-rabbit Alexa Fluor 594 IgG secondary antibody (Life Technologies, A21207) diluted 1:500 in BD perm/wash buffer for 30 min at RT, protected from light. Cells were centrifuged at 1200 rpm for 5 min, washed in BD perm/wash buffer, resuspended in 0.5 mL flow cytometry staining buffer (eBioscience, 00-4222-26) and transferred to BD TruCount tubes (BD Biosciences, 340334, San Jose CA). Samples were run on a special order BD LSRII flow cytometer configured with a 405 nm, 488 nm, 532 nm, and 640 nm laserline using BD FACS Diva 8.0.1 software. Data were analyzed in Kaluza 1.3 (Beckman Coulter). For all antibodies we used fluorescence minus one (FMO) staining and the corresponding isotype controls to determine positive staining from background. For quantification of nucleated cells DAPI (ThermoFisher Scientific, 62248, 1mg/mL) 1:1000 dilution was added to the corresponding samples 15 min prior to analysis.

1.2.8 Proliferation Assay

To detect proliferation of cortical cells *in vivo*, mice were treated with 3 single daily injections (i.p.) 50 mg/kg EdU (Molecular Probes by Life Technologies, E10187) on days 1, 2 and 3 (after injury) for animals processed 3 dpi and on days 2, 4, and 6 for animals processed 7 dpi with the Click-it A647 EdU labeling kit (Molecular Probes by Life Technologies, C10634) for flow cytometry. EdU staining was performed according to manufacturer's instructions after CD309 intracellular staining on fixed and permeabilized cells. Following this step, cells were transferred to BD TruCount tubes and analyzed as described above.

1.2.9 Western Blot Analyses

The ipsilateral cortex of sham and CCI injured animals (3 and 7 dpi) was homogenized in radio-immunoprecipitation assay (RIPA) buffer with protease and phosphatase inhibitor

cocktail (Sigma-Aldrich, St. Louis, MO) and benzonase nuclease (Millipore Corporation, Billerica, MA) and mixed by rocking at 4°C for at least 15 min. After the tissue was centrifuged, the supernatant was collected and the samples were diluted and standardized to protein concentrations. Protein samples were separated on 8% SDS-PAGE gel and transferred to a nitrocellulose membrane. The membranes were then blocked with 5% milk in 0.1 M phosphate buffer with 0.1% Tween-20 for 1 h at RT and incubated overnight at 4°C with primary antibodies. The membranes were then incubated for 1 h at RT with HRP-conjugated secondary antibodies (Jackson Immunoresearch Laboratories, West Grove, PA). Bands were visualized using SuperSignal substrate (ThermoScientific, Pittsburg, PA). The following primary antibodies were used: anti-VEGFR-2 1:200 (Cell Signaling, 2479L), anti-PECAM-1 1:100 (Santa Cruz, SC-1506), anti-VE-Cadherin 1:200 (Santa Cruz, SC-28644) and anti-β-tubulin 1:30,000 (Sigma-Aldrich, T4026), all diluted in 5% milk. ImageJ was used to perform density analysis. Protein measurements were standardized to β-tubulin and normalized to average WT sham signals.

1.2.10 Statistical analysis

Cell populations from CCI injured and sham animals were compared via unpaired two-tailed Student's *t*-test with 95% confidence interval. Significant group differences were reported * $p<0.05$, ** $p<0.01$, *** $p<0.001$ as compared with non-injured mice. Differences between sham and different time points after CCI injury were compared using One-way ANOVA with Bonferroni's post-hoc test in the case of significance (## $p<0.01$, ### $p<0.001$ as compared with 3 dpi injured group). For all graphs, error bars represent ±1 standard error of the mean (SEM). All statistical analyses were performed with GraphPad Prism software, version 5.0. $P<0.05$ were considered significant for all comparisons.

1.3 Results

1.3.1 Controlled cortical impact (CCI) injury leads to progressive tissue and vascular damage

Our primary goal is to establish an efficient flow cytometric method for assessing changes in cortical vascular endothelial cell (cvEC) population after TBI; however, these methods may be used for multiple cell types in the CCI injured brain. It is important to first define the degree of CCI injury using graded velocities to determine the extent of vascular damage and tissue loss in the mouse cortex. Mice were subjected to CCI injury with impact velocities of 2, 4 and 6 m/s and gross tissue damage was evaluated in Hematoxylin and Eosin (H&E) stained coronal brain sections at 3 and 7 days post-injury (dpi). We observed little to no gross tissue damage at 2 m/s at 3 dpi, while 4 and 6 m/s showed graded and progressive tissue damage to the cortex and some subcortical regions (Fig. 1a–f). Despite the absence of gross tissue damage at 3 dpi, vascular damage was observed in the mildest 2 m/s velocity tested (Fig. 1g–j). Analysis of 2 m/s CCI injury in Cdh5-zG mice (endothelial cells labeled in green) showed significant absence of signal at the injury epicenter at 3 dpi (Fig. 1g, h). Infusion of lectin-594 (red) in Cdh5-zG mice to trace infusible vessels confirmed the preservation of cvECs in the injury penumbra (arrow heads) and the absence of vessel in the injury epicenter at 3 dpi (Fig. 1i–j). A similar loss in vessels was observed in the cortex for impact velocities of 4 and 6 m/s with a graded increase in the injury epicenter and penumbra

that matched velocity intensity. For the experiments described in this study, we analyzed endothelial cells in a progressive moderate 4 m/s injured cortex that included a defined tissue epicenter and penumbra for all flow cytometric experiments.

1.3.2 Gating strategy for examining cvECs and EPCs in the injured cortex by flow cytometry

To assess cell viability between injured and non-injured tissues using flow cytometry, we stained cortical cells with a Live/Dead fixable near-IR (L/D) stain, an amine reactive dye that binds proteins and works well for live as well as fixed and permeabilized cells. Initially, dissociated CCI injured tissues were gated on a forward by side scatter plot to exclude cellular debris from the analysis (Fig. 2a). A population of single cells (i.e. singlets) were then selected by homogeneity of size and granularity using forward and side scatters, respectively (not shown). The L/D stain showed reproducible bi-phasic peaks allowing for a clear separation between a viable (left gated, negative) and non-viable cell population (Fig. 2b), where over 80% of single cells were viable. To provide confirmation that viable cells are nucleated, 4’,6-Diamidino-2-Phenylindole, Dihydrochloride (DAPI) was applied following fixation showing an uniform bell shape curve with nucleation of nearly the entire population (97%; Fig. 2c). In addition to cell loss after CCI injury, cell infiltration and differentiation can also alter the overall makeup of the injured cortex, and cell specific markers may label multiple populations (Jin X *et al.*, 2012). CD31 (PECAM-1) is widely accepted as an endothelial cell (EC) marker, where FITC-conjugated CD31 antibody labeled large populations of viable cells in both sham and CCI-injured mice at 7 dpi (Fig. 2d). Since CD31 is also expressed by hematopoietic cells including monocytes and macrophages that can potentially infiltrate into the injured cortex, CD45 (leukocyte common antigen) was used as an exclusion marker to eliminate infiltrating leukocytes as well as residential microglia from the analysis. We observed a significant 54% reduction in the number of $CD45^{-}/CD31^{+}$ cells in CCI-injured animals compared with sham controls (Fig. 2d), which was observed only following CD45 exclusion. These reductions support the qualitative histological losses in cvECs observed (Fig. 1).

To better evaluate cell infiltration in the cortex, we examined the differences between $CD45^{+}$ and $CD45^{-}$ cells at 3 and 7 dpi compared to non-injured animals (Fig 2e–h). In non-injured conditions, we found that over 67% of viable cells are $CD45^{-}$, while approximately 31% are $CD45^{+low}$ (microglia) and <2% are $CD45^{+high}$ (infiltrating leukocytes). At 3 and 7 dpi, we observe a significant decrease in $CD45^{-}$ cells accompanied by an increase in $CD45^{+}$ cells compared with non-injured controls. The $CD45^{+low}$ and $CD45^{+high}$ populations increase to 53% and 13%, respectively, of total viable cells at 3 dpi, and although the percentage of $CD45^{+low}$ cells remains high by 7 dpi (53%, Fig 2h), the percent of $CD45^{+high}$ cells returns to non-injured levels (~2%). Since CD31 is also expressed by both mature residential cvECs and bone marrow derived endothelial progenitor cells (EPCs), the cvEC marker CD144 (VE-Cadherin) was also used. BV421-conjugated CD144 antibody distinctly labels mature cvECs ($CD45^{-}/CD144^{+}$) (Fig. 2i) compared to its isotype control (Fig. 2k). To examine EPCs, vascular endothelial growth factor receptor 2 (VEGFR-2 or CD309) was used in combination with the progenitor marker prominin-1 (CD133) for labeling EPCs out of the $CD45^{-}/CD144^{-}$ population (identified as $CD45^{-}/CD144^{-}/CD309^{+}/CD133^{+}$) (Fig. 2j)

against the isotype control (Fig. 2l). Figure 2m shows that $CD144^+$ mature cvECs represents 57% of the $CD45^-$ population, whereas $CD144^-/CD309^+/CD133^+$ EPCs represent only 1% of the $CD45^-$ population. Given that CD133 has very low expression levels and $CD133^+$ EPCs represent a very small percentage of the total endothelial cell population we used an isotype control to facilitate gating on $CD133^+$ cells in combination with a phycoerythrin (PE)-conjugated, a bright fluorescent dye with a high staining index, anti-CD133 antibody. Although very bright, PE has a similar absorbance wavelength to blood erythrocytes. Thus, to evaluate whether erythrocytes interfered with the intensity of PE fluorescence, we examined PE intensity levels in the presence and absence of blood. We observed no significant differences in the background of the PE channel compared to its isotype control between perfused and non-perfused brains, suggesting that the number of erythrocytes in the brains were not significant to dim the PE intensity in our samples (Suppl. Fig. 1). At 7 dpi, the percentage of mature cvECs (51.8%) was not significantly different from non-injured controls. The percentage of EPCs was significantly increased ($p<0.001$) at 7 dpi to 2% of the $CD45^-$ population (Fig. 2m). While these findings support an increase in the EPC population after CCI injury, they do not support the visible losses in cvECs observed in cortical tissues (Fig. 1), suggesting that the percent of intergroup variance using flow analysis is not an accurate measurement of cell numbers after CCI injury. To better address cell changes after injury, quantification of actual cell numbers is required.

1.3.3 Quantification of endothelial cell numbers after TBI using TruCount beads

TBI results in a constantly changing environment due to the large amount of cell death, peripheral infiltration, and proliferation that take place after injury. This multitude of cellular redistribution in the injured brain increases the potential variability between animals, but also invalidates comparisons of the percent of total cells between sham and injured tissues. In fact, many flow cytometers read a fixed number of events that cap their readings, irrelevant of the volume analyzed, to determine the percent of cells within a given total fixed number of events. Comparison of $CD45^-/CD144^+$ cells between sham and CCI tissues show no significant difference at 7 dpi (Fig. 3a); however, this doesn't reflect the observed vascular pathology associated with the absence of cvECs after CCI injury (Fig. 1h). To ensure that we have consistency and accurate counts of specific cell populations, we quantified the number of cells per volume of sample using BD TruCount tubes. TruCount tubes contain an absolute number of fluorescent beads per tube, where the number of cells per volume can be calculated. Basically, the number of fluorescent beads analyzed per total events is determined for each sample by placing a gate around the beads which, on our system, consistently appear on the top left hand corner of the scatter plot (Fig. 3b). A known volume of sample (500μL) is added to each individual TruCount tube and the volume analyzed (Va) can be computed by dividing the number of beads analyzed by the total beads in the tube and multiplied by the sample volume. Once the Va is known, the number of cells per volume of sample (cells/μL) can be quantified by dividing the number of events within each desired gate by the Va.

$$\mathrm{Va} = [\text{analyzed beads}]/[\text{total beads}] * \text{original volume}$$
$$\mathrm{Cells}/\mu\mathrm{L} = [\text{gated evevts}]/[\mathrm{Va}]$$

Re-examining the same $CD45^{-}/CD144^{+}$ population now shows a significant decrease at 7 dpi when analyzed as either fold change from the contralateral control cortex (Fig. 3c) or determination of actual cortical cvEC number per volume of sample (cells/μL) (Fig. 3d). These findings are consistent with observed cvEC losses since they take into consideration total cell losses, cell infiltration and proliferation known to take place at these early time points after TBI (Greve and Zink, 2009) (Fig. 2e–h). Smaller discrepancies are observed when analyzing larger cell populations, such as the $CD45^{+}$ cells, where increases in cell percent, fold change, and cell numbers are still observed (Fig. 3 e–g). This was confirmed in a non-infiltrating and non-proliferating neuron population, where Thy-1-YFP transgenic mice were used to examine the effects of CCI injury on cortical neuron numbers. Our samples showed a distinct population of YFP^{+} cells gated out of viable $CD45^{-}$ singlets (Fig. 3h) that were evaluated using percent comparison to total cells versus TruCount analysis, where neuron cell losses at 7 dpi were only observed using TruCount analysis (Fig. 3i–k). All subsequent experiments employ TruCount beads for analysis.

1.3.4 In-vivo assessment of cell proliferation after CCI injury using EdU and flow cytometry

Cell proliferation accounts for one of the constantly changing components after TBI. Quantification of proliferating cells can be challenging using conventional immuno-histochemical methods where confocal imaging and stereological counts might be labor intensive. To determine whether cell proliferation of individual cell populations could be assessed by flow cytometry in our TBI model, CCI-injured and sham mice were pulsed with EdU for the first 3 days after injury and the brains were processed for either immunohistochemistry (IHC) or flow cytometry using a click-it EdU assay kit at 3 and 7 dpi. Confocal images of Cdh5-zG brains showed a dramatic increase in EdU^{+} cells (red) around blood vessels (green) at the injury penumbra during the first 3 days after injury when compared to non-injured sham controls (Fig. 4 a–b). Consistently, flow histograms also showed a significant increase in total cell proliferation at 3 dpi with approximately 20% more total viable EdU^{+} cells after injury compared with non-injured animals (Fig. 4 c–d). *In vivo* assessment of proliferating cvEC and EPC populations using flow cytometry was computed by first quantifying the TruCounts for each individual cell type as well as the number of EdU^{+} cells within each gate. The percent of EdU^{+} cells was then computed as a ratio of the total cells for each population of interest at both 3 and 7 dpi. The internal control leukocyte common antigen marker, CD45, showed dramatic increases in proliferation at both time points, while YFP^{+} neurons showed no change in proliferation after CCI injury (Fig. 4e). When quantifying proliferation of the endothelial populations, both the cvECs and EPCs showed a significant increase in the ratio of EdU^{+} cells out of the total cell populations at 3 and 7 dpi, with the great majority of proliferation (over 20%) occurring at the earlier time point for EPCs (Fig. 4 f). Thus, flow cytometry provides a reliable tool for analyzing multiple conditions and cell types in the complex TBI environment.

1.3.5 Evaluation of protein expression levels by Mean Fluorescence Intensity (MFI) using flow cytometry

In addition to cell numbers, flow cytometry can also provide a measurement of protein expression levels by mean fluorescence intensity (MFI). MFI provide a means to determine the average level of expression per cell for a particular protein of interest. To determine

whether MFI is a reliable measure of protein expression, we compared three different endothelial proteins, PECAM-1, VEGFR-2, and VE-Cadherin at 3 and 7 dpi using flow cytometry and western blot analysis (Fig. 5). Our results show a similar trend between the two methods for all three proteins of interest although we observed differences in fold change, which could be attributed to examination of MFI per cell versus whole tissue analysis. Temporal analysis shows a significant increase in PECAM-1, VEGFR-2, and VE-Cadherin at 3 dpi which then returns to sham levels by 7 dpi (Fig. 5a–f). The only exception was VEGFR-2 that remained significantly high at 7 dpi (Fig. 5c, d).

1.4 Discussion

This study examines the complex nature of traumatic brain injury (TBI) where cell death, proliferation and invasion all participate in defining the progressive pathology associated with injured tissues. Flow cytometry can be a powerful tool to examine the changes of multiple cell types after TBI; however, comparison over time and with non-injured sham controls can be difficult to interpret. Here, we examine two cell populations involved in the cerebral vascular network, namely cerebral vascular endothelial cells (cvECs) and endothelial progenitor cells (EPCs), following a murine controlled cortical impact (CCI) injury. This report examines how investigators can accurately quantify cell changes after CCI injury using a conventional flow cytometer that “caps events” during cell analysis. We show that employing a single platform volumetric standard, i.e. TruCount beads, provides an accurate method to quantify cell numbers as opposed to analyzing events or gated percent of viable cells. Using TruCount methods, our results demonstrate that the cvEC population ($CD45^{-}/CD144^{+}$ cells) is significantly reduced at 3 dpi, whereas the EPC population ($CD309^{+}/CD133^{+}$ cells) is significantly increased. Although the EPC population represents only a small percent of total cortical cells, a greater percent of EPCs are actively proliferating as compared to cvECs in the first week post-injury. These studies also demonstrate that protein expression levels can be measured using flow cytometry by examining the mean fluorescent intensity (MFI) per cell. The average levels of PECAM-1, VEGFR-2 and VE-Cadherin are significantly upregulated in $CD45^{-}$ cells, including cvECs and EPCs, at 3 dpi, which reflect a period when the blood brain barrier (BBB) is disrupted. MFI analysis could also provide more meaningful expression data within a specific cell population since it only evaluates the average protein levels per living cell, while analysis of whole tissue samples using Western blot possibly reflects multiple cell types as well as proteins in dead or dying cells in the CCI injured brain. Overall, these studies demonstrate that flow cytometry can be a useful tool for analyzing temporal changes in protein levels and cell populations within the complex pathology of the injured brain.

The development of more sophisticated flow cytometers have permitted investigators to measure exact sample volumes to accurately determine cell numbers; however, the more common conventional flow cytometers cap events read at a specific number irrespective of the volume analyzed. For this reason, the conventional approach is to measure cells of interest as a percent of total capped viable cells. Unfortunately, we show that analyzing percent cell changes between injured tissues and non-injured controls can be misleading or even dramatically incorrect, which is especially concerning when analyzing small cell populations. These discrepancies result from dramatic environmental changes in the

traumatic injured brain, where residential cells undergo progressive cell death, subpopulations of cells initiate proliferation and differentiation processes, and infiltrating cells (mainly $CD45^+$ cells) enter the CNS through a disrupted BBB. These differences make it difficult to compared CCI injured tissues with sham controls. To overcome this problem, we took advantage of TruCount beads, where a fixed sample volume is added to TruCount tubes containing a set number of fluorescently labeled beads, so that the volume analyzed per sample by the flow cytometer can be computed by determining the number of beads analyzed. Thus, the number of cells per microliter can be determined irrespective of variability in total cell number or volume analyzed. The most convincing evidence for this differential effect was our analysis of residential cortical neurons, where conventional analysis comparing the percent of YFP^+ cells to total viable cells resulted in a significant increase in neurons at 3 dpi. Examining the same data using TruCounts showed the opposite trend where the number of YFP^+ neurons was significantly reduced after CCI injury, which supports the well-known fact that CCI injury leads to acute neuronal loss (Chen et al., 2003; Zhang et al., 2005).

Another approach to overcoming the complications related to infiltrating cells is to isolate the cells of interest using column purification methods or panning methods prior to flow analysis. This may be an important step for FACS sorting but a strength of using flow cytometry in the TBI model is to examine multiple cell types at a given time point to better understand the overall pathological process and tissue environment. In addition, the more involved the methods are for preparing tissue sample for flow analysis, the greater amount of error is introduced for accurate cell quantification. We compared samples with and without exclusion of myelin and tissue debris, and found that exclusion of myelin/tissue debris is important for reducing fluorescent background especially when analyzing smaller cell populations. Other investigators have taken an additional step to avoid non-specific antibody binding by removing phagocytic cells, such as macrophages, that also express Fc receptors and are prone to false positive staining (Wylot et al., 2015). Depletion of $CD11b^+$ microglia/macrophages will improve the purity of cvECs; however, invasion of macrophages and reactivity of microglia cells are significant parts of TBI pathology. Furthermore, the additional purification steps also reduce the accuracy of cell quantification. We account for these potential false positives by first blocking non-specific Ig binding with FcR blocking solution and using a common leukocyte antigen antibody (CD45) as an exclusion marker. This approach provides a better understanding of the temporal dynamics of multiple cell populations within the traumatically injured brain.

For the past several decades investigators have examined the cerebral energy input, alterations in cerebral blood flow, cerebral metabolic dysfunction, imbalanced cerebral oxygenation, and increased BBB permeability in multiple CNS injury models (Immonen et al., 2010; Kan et al., 2012; Lin et al., 2012; Toklu and Tumer, 2015). Fewer studies have examined the cellular changes that underlie these functional deficits, where endothelial cells make up the lumen of blood vessels. In a rat CCI injury model, Chen and colleagues report an overall reduction in blood vessel density in the peri-lesional cortex at 1, 4, and 7 dpi (Chen et al., 2003). These findings are consistent with our observed reductions in blood vessels in the injury epicenter and cvEC numbers in the cortex. Our observed increase in EPC numbers after CCI injury in mice is also consistent with previous TBI studies in rats

where EPCs are increased between 1 and 3 dpi (Guo et al., 2009), and in humans where increased circulating EPCs are observed in the first week in TBI patients (Liu et al., 2007). The advantage of flow cytometry analysis is our ability to quantify both cell types within the entire cortex in relationship with each other and their quiescent or proliferative states.

Endothelial proliferation and EPC invasion are thought to contribute to vessel repair and/or regeneration after TBI (Chen et al., 2013; Guo et al., 2009; Melero-Martin et al., 2007). Ischemic models of CNS injury have demonstrated that ECs have the potential to proliferate after injury (Hayashi et al., 2003); however, few studies have addressed EC expansion after TBI. Our studies examined individual cell types using the 5-ethynyl-2′-deoxyuridine (EdU) incorporation as a proliferative marker where we observed expansion of both mature cvECs and infiltrated EPCs in the CCI injured cortex. The proliferation of ECs is consistent with previous observations in rat TBI models (Morgan et al., 2007; Nag et al., 1997). Our findings demonstrate that expanding cvECs and EPCs may participate in vessel repair in the first week post-injury, while the expansion of $CD45^+$ cells may also influence recovery. In addition to proliferation, cell death can have important implications on tissue analysis and TBI progression. Our attempt to validate apoptotic cells within the CCI injured cortex using either the live/dead stain or a Cell Event Caspase-3/7 Green Flow Cytometry Assay kit were inconsistent. We believe these inconsistencies resulted from the exclusion of dying cells during the tissue dissociation process and staining procedures where cells undergo multiple centrifugations and washing steps. For these reasons, within our experimental constraints we were unable to accurately assess the number of dead and apoptotic cells. Together, our findings reflect the complex nature of TBI, where it is important to enhance the expansion of subpopulations of cells, such as progenitor cells and vascular cells, but it may be less desirable to expand certain populations of peripheral leukocytes.

Supplementary Material

Refer to Web version on PubMed Central for supplementary material.

Acknowledgments

We thank Melissa M. Carballosa-Gautam in the microscopy core facilities at the Miami Project to Cure Paralysis. We also thank Dr. Yanina Tsenkina for critical reading of our manuscript and Jose Mier for assistance with animal husbandry. This work was supported by the Miami Project to Cure Paralysis, NIH/NINDS NS049545 (DJL), NS30291 (DJL), F31NS089325-01 (PAN) and the Lois Pope Life fellowship (PAN).

Abbreviations

BABB	Benzyl alcohol, benzyl benzoate
BBB	Blood-brain barrier
BSA	Bovine serum albumin
Cdh-5	Cadherin
CNS	Central nervous system
cvEC	Cerebral vascular endothelial cell

CCI	Controlled cortical impact
cc	Corpus callosum
Ctx	Cortex
dpi	Days post-injury
EC	Endothelial cell
EPC	Endothelial progenitor cell
EtOH	Ethanol
FMO	Fluorescence minus one
H&E	Hematoxylin and eosin
Hipp	Hippocampus
IHC	Immunohistochemistry
i.p	Intraperitoneal injections
L/D	Live/Dead
MFI	Mean Fluorescence Intensity
PFA	Paraformaldehyde
PECAM-1	Platelet endothelial cell adhesion molecule
PBS	Phosphate buffered saline
PE	Phycoerythrin
RIPA buffer	Radioimmunoprecipitation assay
SEM	Standard error of the mean
TBI	Traumatic brain injury
VEGFR-2	Vascular endothelial growth factor receptor
VE-Cadherin	Vascular endothelial
Th	Thalamus
THF	Tetrahydrofuran
Va	Volume analyzed
YFP	Yellow fluorescent protein
DAPI	4′,6-diamidino-2-phenylindole
EdU	5-ethynyl-2′-deoxyuridine

References

Abbott NJ, Patabendige AA, Dolman DE, Yusof SR, Begley DJ. Structure and function of the blood-brain barrier. Neurobiology of disease. 2010; 37:13–25. [PubMed: 19664713]

Abdul-Muneer PM, Schuetz H, Wang F, Skotak M, Jones J, Gorantla S, Zimmerman MC, Chandra N, Haorah J. Induction of oxidative and nitrosative damage leads to cerebrovascular inflammation in an animal model of mild traumatic brain injury induced by primary blast. Free radical biology & medicine. 2013; 60:282–291. [PubMed: 23466554]

Bendall SC, Nolan GP, Roederer M, Chattopadhyay PK. A deep profiler's guide to cytometry. Trends Immunol. 2012; 33:323–332. [PubMed: 22476049]

Centers for Disease, C., and Prevention. CDC grand rounds: reducing severe traumatic brain injury in the United States. MMWR Morbidity and mortality weekly report. 2013; 62:549–552. [PubMed: 23842444]

Chen S, Pickard JD, Harris NG. Time course of cellular pathology after controlled cortical impact injury. Experimental neurology. 2003; 182:87–102. [PubMed: 12821379]

Chen X, Yin J, Wu X, Li R, Fang J, Chen R, Zhang B, Zhang W. Effects of magnetically labeled exogenous endothelial progenitor cells on cerebral blood perfusion and microvasculature alterations after traumatic brain injury in rat model. Acta radiologica. 2013; 54:313–323. [PubMed: 23528570]

Das M, Mohapatra S, Mohapatra SS. New perspectives on central and peripheral immune responses to acute traumatic brain injury. Journal of neuroinflammation. 2012; 9:236. [PubMed: 23061919]

De Rosa SC, Herzenberg LA, Herzenberg LA, Roederer M. 11-color, 13-parameter flow cytometry: Identification of human naive T cells by phenotype, function, and T-cell receptor diversity. Nat Med. 2001; 7:245–248. [PubMed: 11175858]

Greve MW, Zink BJ. Pathophysiology of traumatic brain injury. The Mount Sinai journal of medicine, New York. 2009; 76:97–104.

Guo X, Liu L, Zhang M, Bergeron A, Cui Z, Dong JF, Zhang J. Correlation of CD34+ cells with tissue angiogenesis after traumatic brain injury in a rat model. Journal of neurotrauma. 2009; 26:1337–1344. [PubMed: 19226208]

Hayashi T, Noshita N, Sugawara T, Chan PH. Temporal profile of angiogenesis and expression of related genes in the brain after ischemia. Journal of cerebral blood flow and metabolism : official journal of the International Society of Cerebral Blood Flow and Metabolism. 2003; 23:166–180.

Immonen R, Heikkinen T, Tahtivaara L, Nurmi A, Stenius TK, Puolivali J, Tuinstra T, Phinney AL, Van Vliet B, Yrjanheikki J, Grohn O. Cerebral blood volume alterations in the perilesional areas in the rat brain after traumatic brain injury--comparison with behavioral outcome. Journal of cerebral blood flow and metabolism : official journal of the International Society of Cerebral Blood Flow and Metabolism. 2010; 30:1318–1328.

Jin X, Ishii H, Bai Z, Itokazu T, Yamashita T. Temporal changes in cell marker expression and cellular infiltration in a controlled cortical impact model in adult male C57BL/6 mice. PLoS One. 2012; 7:e41892. [PubMed: 22911864]

Kan EM, Ling EA, Lu J. Microenvironment changes in mild traumatic brain injury. Brain research bulletin. 2012; 87:359–372. [PubMed: 22289840]

Lin Y, Pan Y, Wang M, Huang X, Yin Y, Wang Y, Jia F, Xiong W, Zhang N, Jiang JY. Blood-brain barrier permeability is positively correlated with cerebral microvascular perfusion in the early fluid percussion-injured brain of the rat. Laboratory investigation; a journal of technical methods and pathology. 2012; 92:1623–1634.

Liu L, Liu H, Jiao J, Liu H, Bergeron A, Dong JF, Zhang J. Changes in circulating human endothelial progenitor cells after brain injury. Journal of neurotrauma. 2007; 24:936–943. [PubMed: 17600511]

Lugli E, Roederer M, Cossarizza A. Data Analysis in Flow Cytometry: The Future Just Started. Cytom Part A. 2010; 77A:705–713.

Mair F, Hartmann FJ, Mrdjen D, Tosevski V, Krieg C, Becher B. The end of gating? An introduction to automated analysis of high dimensional cytometry data. Eur J Immunol. 2016; 46:34–43. [PubMed: 26548301]

Melero-Martin JM, Khan ZA, Picard A, Wu X, Paruchuri S, Bischoff J. In vivo vasculogenic potential of human blood-derived endothelial progenitor cells. Blood. 2007; 109:4761–4768. [PubMed: 17327403]

Morgan R, Kreipke CW, Roberts G, Bagchi M, Rafols JA. Neovascularization following traumatic brain injury: possible evidence for both angiogenesis and vasculogenesis. Neurological research. 2007; 29:375–381. [PubMed: 17626733]

Nag S, Takahashi JL, Kilty DW. Role of vascular endothelial growth factor in blood-brain barrier breakdown and angiogenesis in brain trauma. Journal of neuropathology and experimental neurology. 1997; 56:912–921. [PubMed: 9258261]

Perfetto SP, Chattopadhyay PK, Roederer M. Innovation - Seventeen-colour flow cytometry: unravelling the immune system. Nat Rev Immunol. 2004; 4:648–U645. [PubMed: 15286731]

Sorensen I, Adams RH, Gossler A. DLL1-mediated Notch activation regulates endothelial identity in mouse fetal arteries. Blood. 2009; 113:5680–5688. [PubMed: 19144989]

Timmermans F, Plum J, Yoder MC, Ingram DA, Vandekerckhove B, Case J. Endothelial progenitor cells: identity defined? Journal of cellular and molecular medicine. 2009; 13:87–102. [PubMed: 19067770]

Toklu, HZ.; Tumer, N. Oxidative Stress, Brain Edema, Blood-Brain Barrier Permeability, and Autonomic Dysfunction from Traumatic Brain Injury. In: Kobeissy, FH., editor. Brain Neurotrauma: Molecular, Neuropsychological, and Rehabilitation Aspects. Boca Raton (FL): 2015.

Wylot B, Konarzewska K, Bugajski L, Piwocka K, Zawadzka M. Isolation of vascular endothelial cells from intact and injured murine brain cortex-technical issues and pitfalls in FACS analysis of the nervous tissue. Cytometry Part A : the journal of the International Society for Analytical Cytology. 2015; 87:908–920. [PubMed: 25892199]

Xue S, Zhang HT, Zhang P, Luo J, Chen ZZ, Jang XD, Xu RX. Functional endothelial progenitor cells derived from adipose tissue show beneficial effect on cell therapy of traumatic brain injury. Neuroscience letters. 2010; 473:186–191. [PubMed: 20178832]

Zhang X, Chen Y, Jenkins LW, Kochanek PM, Clark RS. Bench-to-bedside review: Apoptosis/programmed cell death triggered by traumatic brain injury. Critical care. 2005; 9:66–75. [PubMed: 15693986]

Highlights

- TruCount beads and flow cytometry can accurately quantify multiple cells in cortex.
- Residential cvECs are reduced, while invading EPCs are increased after TBI.
- Proliferation of cvECs and EPCs support reparative processes in the injured brain.
- Analysis of mean fluorescent intensity quantifies protein levels in specific cells.
- Our method provides a new comprehensive approach to examining cvECs and EPCs after TBI.

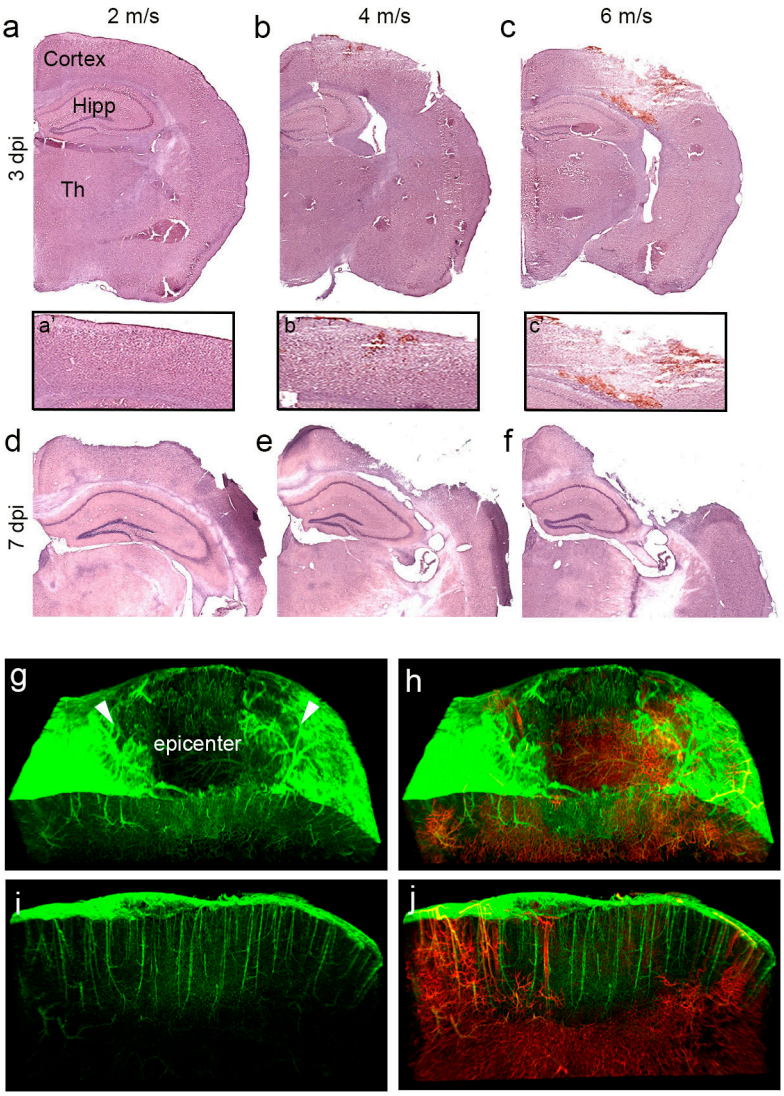

Figure 1.

Graded CCI injury leads to graded cortical damage and vascular loss at the injury epicenter. (a–f) Hematoxylin and eosin (H&E) stained coronal brain sections at impact velocities of 2 m/s (a, d), 4 m/s (b, e), and 6 m/s (c, f) at 3 (a–c) and 7 (d–f) days after CCI injury (dpi). (a′–c′) Higher magnification H&E stained images of injured cortex. (g–j) Light-sheet 3D images of the CCI injured cortex at 3 dpi in Cdh5-zG mice infused with Lectin-594. Arrowheads depict injury penumbra. Sagittal view of the injury penumbra reveals the presence of ECs (i) but not infusible vessels (j). Hipp, hippocampus, Th, thalamus.

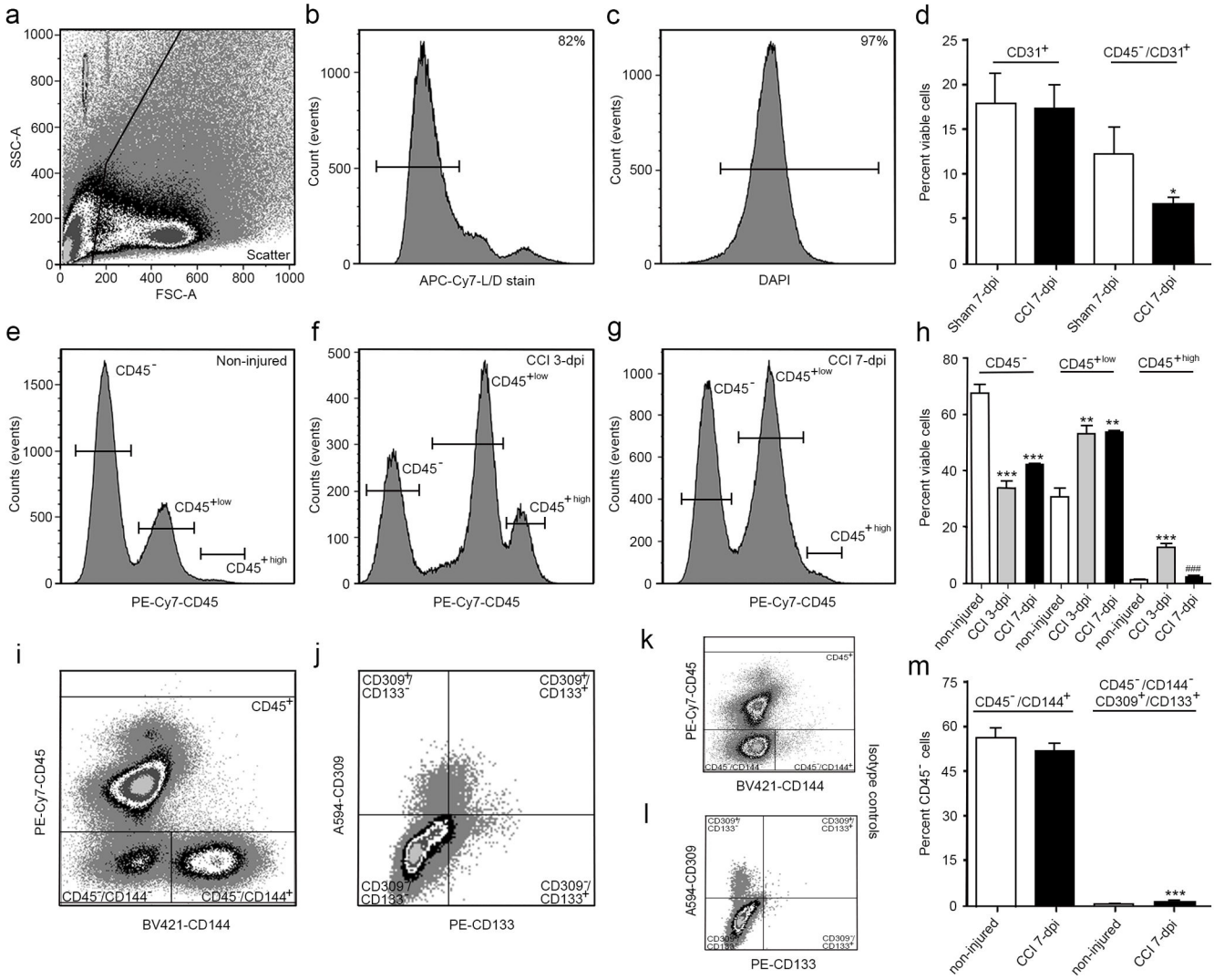

Figure 2.

CCI injury leads to differential changes in the percent of CD45^{-} and CD45^{+} subpopulations of cells in the cortex. (a) Scatter plot shows exclusion of cellular debris. Viable (b) and nucleated (c) cells were selected for using a live/dead stain followed by DAPI staining. (d) No difference was observed in viable CD31^{+} (PECAM-1) cells between sham and CCI-injured mice at 7 dpi; however, excluding CD45^{+} cells from the analysis results in a significant decrease in CD45^{-}/CD31^{+} cvECs. (e–h) CCI injury increased the percent of CD45^{high} (infiltrating leukocytes) and CD45^{low} (residential microglia), while reducing the population of CD45^{-} cells. (i) Scatter plot showing separation of CD144^{+} (VE-cadherin) cvECs, and CD309^{+} (VEGFR-2)/CD133^{+} (Prominin-1) EPCs (j). Scatter plot showing isotype controls for CD45^{-}/CD144^{+} (k) and CD309^{+}/CD133^{+} (l) populations. (m) At 7 dpi the percentage of CD45^{-}/CD144^{+} ECs was not changed whereas the smaller CD309^{+}/CD133^{+} EPC population was significantly increased. n=3 biological replicates. * $p<0.05$, ** $p<0.01$, *** $p<0.001$ as compared with non-injured mice.

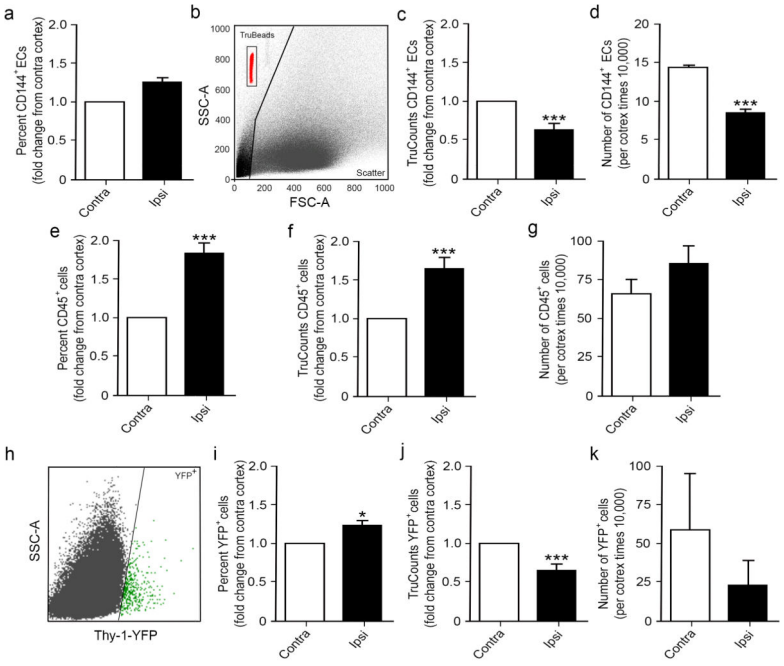

Figure 3.

TruCount beads provide an accurate method for quantifying cortical cell numbers at 7 dpi. (a) Percent of $CD144^+$ cvECs was unchanged in the ipsi versus contralateral cortex. (b) Scatter plot of TruCount beads (red) shows a distinct separation from cells. Quantification of $CD144^+$ cvECs using TruCount beads revealed a significant decrease in both the fold change (c) and actual cell numbers (d) compared with the contralateral cortex. (e–g) Analysis of a large $CD45^+$ cell population shows a similar increase in the ipsilateral injured cortex as compared with the contralateral cortex using percent change (e) and fold change based on TruCount beads (f) or cell number (g) analysis; however, the values are different between methods. (h) Scatter plot of Thy-1-YFP fluorescing neurons (green) show distinct population of cells. (i–k) Opposite results were observed in this smaller control population of cells where percent change (i) was increased, while TruCount analysis showed decreases in fold change (j) or cell numbers (k). (a, c–g) n=9; (i–k) n=6. * $p<0.05$, *** $p<0.001$ as compared with contralateral cortex.

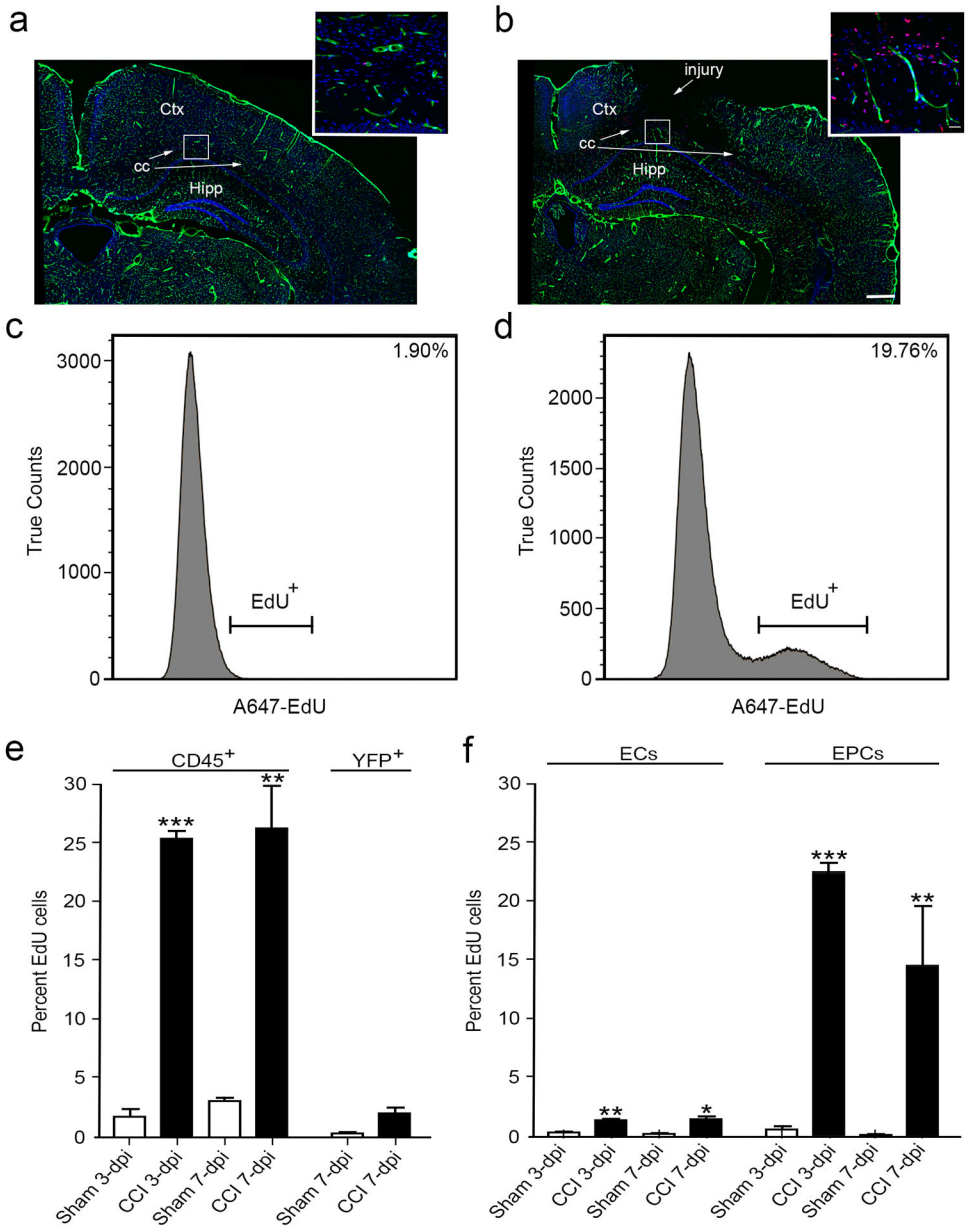

Figure 4.

Proliferating EdU+ infiltrating cells ($CD45^+$), cvECs and EPCs are increased at 3 and 7 dpi. (a) Immunostained coronal brain section of non-injured sham Cgh5-zG (green) cortex shows DAPI staining (blue) and few proliferating cells (red). Inset is a high-magnification image of subcortical layers. (b) Immunostained coronal brain section of CC-injured Cgh5-zG (green) cortex at 3 dpi shows DAPI staining (blue) and greater numbers of proliferating cells (red). Inset is a high-magnification image of subcortical layers in the penumbra. (c, d) Flow cytometry analysis revealed a nearly 20% increase in total viable EdU^+ cells at 3 dpi (d) compared with sham (c) mice. (e) $CD45^+$ infiltrating cells were significantly proliferating at 3 and 7 dpi, while YFP^+ neurons were not proliferating. (f) cvEC and EPC were significantly proliferating at 3 and 7 dpi. (a, b) n=3; (c–f) n=9–12. ** $p<0.01$, *** $p<0.001$

as compared with non-injured sham mice. Ctx, cortex; cc, corpus callosum; Hipp, hippocampus.

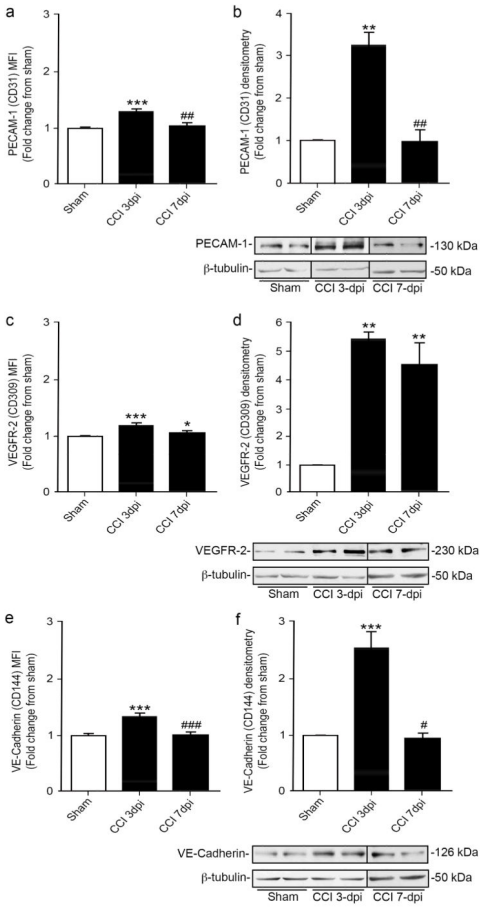

Figure 5.

Changes in protein expression after CCI injury measured as Mean Fluorescence Intensity (MFI) by flow cytometry is consistent with Western blot analysis of the whole cortex. The expression of endothelial proteins PECAM-1 (CD31) (a, b), VEGFR-2 (CD309) (c, d), and VE-Cadherin (CD144) (e, f) was measured as change in MFI (a, c, e) and Western blot analysis (b, d, f) at 3 and 7 dpi as compared with sham controls. A significant increase was observed in the expression of all three proteins analyzed at 3 dpi followed by a significant decrease for both PECAM-1 (a–b) and VE-Cadherin (e–f) at 7 dpi. (c, d) VEGFR-2 levels remained significantly increased at 3 and 7 dpi. (a, c, e) n=3–9 biological replicates; b, d, f) n=3 biological replicates. * $p<0.05$, ** $p<0.01$, *** $p<0.001$ as compared with non-injured sham mice. ## $p<0.01$, ### $p<0.001$ as compared with 3 dpi.